

ORGANIC SEMICONDUCTORS AS CANDIDATES FOR ADVANCED OPTOELECTRONIC DEVICES

G. Bratina and R. Hudej

Nova Gorica Polytechnic, Slovenia

INVITED PAPER

MIDEM 2001 CONFERENCE

10.10.01 - 12.10.01, Hotel Zlatorog, Bohinj

Key words: OS, organic semiconductors, optoelectronic devices, ultrathin flexible multicolor displays, LED displays, Light-Emitting Diode displays, FET, Field Effect Transistors, OLED, Organic Light Emitting Diodes, Van der WAALS force, LONDON force, PTEDA, PeryleneTetraCarbox DiAnhydride

Abstract: Organic semiconductors are gaining an increasing attention due to their promise of novel optoelectronic devices. The main attraction of these materials stems from their potential integration with flexible materials, which would result in ultrathin flexible multicolor displays. Basic electronic properties of typical representatives of organic semiconductors are reviewed. The operation of a light-emitting device based on organic semiconductors is fundamentally different from its inorganic counterparts due to differences in electronic transport properties. The crucial component apart from the active material is represented by the metal-organic semiconductor contacts.

Organski polprevodniki - kandidati za napredne optoelektronske komponente

Ključne besede: OS polprevodniki organski, naprave optoelektronske, zasloni večbarvni fleksibilni ultratanki, LED zasloni z diodami svetlobo sevajočimi, FET transistorji z učinkom polja, OLED diode svetlobo sevajoče organske, Van der WAALS sila, LONDON sila, PTEDA perilentetrakarboksilni dianhidrid

Izveček: Interes za organske polprevodnike se povečuje, saj gre za obetaven material, s pomočjo katerega bomo lahko izdelali nove optoelektronske elemente. Glavni čar teh materialov je njihova zmožnost integracije z upogljivimi materiali, kar bi omogočilo izvedbo izredno tankih upogljivih barvnih prikazovalnikov.

V prispevku predstavimo osnovne električne lastnosti tipičnih predstavnikov organskih polprevodnikov. Delovanje svetlečih elementov na osnovi organskih polprevodnikov se v osnovi razlikuje od delovanja njihovih neorganskih dvojnikov zaradi razlik v načinu transporta nabojev. Poleg materiala samega pa predstavlja kontakt kovina - organski polprevodnik naslednji pomemben faktor pri obnašanju komponente.

1. Introduction

Currently, two venues in material science of the organic semiconductors (OS) are being explored. The materials based on small molecules and polymers. The small-molecule materials are typically employed in thin-film-based devices and are synthesized by vacuum evaporation. These materials have relatively low molecular weight (~500 - 2000). Polymer films, on the other hand, are typically fabricated by dip-coating of the substrate, and have considerably higher molecular weight (~10 000 - 100 000). Since the excitation mechanisms are essentially the same for both classes of materials, the choice is a matter of preference of fabrication method. In what follows we will discuss only the small-molecule type of materials.

The most advanced OS-based devices to date are represented by field-effect-transistors (FETs) and organic light emitting diodes (OLEDs). In the early stage of development of OLEDs organic single crystals were employed. Relatively high dielectric constant of these materials forced the use of high voltages to achieve sufficiently high electric fields. High voltages coupled to poor reproducibility in material synthesis procedures and fabrication of metallic

contacts caused extremely low reliability of the first devices. The use of the Langmuir-Blodgett technique yielded considerable improvement since it allowed the fabrication of OS layers with the thickness of well below of a micron.

The development in the OS thin-film fabrication techniques resulted in higher structural quality of the layers. The availability of novel materials resulted in better alignment of the electronic energy levels at the metal-OS interface. Consequently, in late eighties Tang *et al.* /1/ demonstrated OLEDs with efficiency and lifetime that promised the use in lighting and display applications. In by the end of nineties the OLEDs reached the commercialization stage. Further improvement in efficiency was achieved by the Princeton group through the use of fluorescent dye in the multi-layer structure /2/.

2. Organic light-emitting devices

2.1 Basic material properties

OSs exhibit markedly different structural and electronic properties than their inorganic counterparts. The basic building blocks of OS are molecules instead of atoms. The

fundamental intramolecular interaction is Van der Waals or London force. Consequently organic molecular crystals reveal rather weak structure. The main advantage of such bonding is its relatively small modulus of elasticity, which allows the structure to adapt to a variety of different substrates. This is important when we consider the possibility of integrating optoelectronic devices with flexible structures such as plastics.

The main consequence of Van der Waals bonding is small overlap between the electronic wave functions centered on atoms of neighboring molecules. This has profound implications on the transport of the electronic charge in OSs. The absence of extended delocalized states, results in the charge transport that is not coherent in energy bands but stochastic hopping from one localized state to another. Such transport is extremely sensitive to electrically active structural defect that typically act as traps for the carriers, resulting in overall carrier mobilities in the range between 10^{-4} to $1 \text{ cm}^2/\text{Vs}$.

Many of the OSs currently under investigation are wide-gap materials with the energy separation between the highest unoccupied molecular orbital (HOMO) and the lowest occupied molecular orbital (LUMO) of 2-3 eV. This results in a very low concentration of thermally activated carriers. In addition to structural defects also impurities typically act as traps rather than sources of free carriers as in the case of inorganic semiconductors. Frequently oxygen and/or ambient water molecules affect the electronic transport in these materials.

There are several OSs that are employed in OLEDs, most frequently used is aluminum chelate complex (Alq) This is an electron conducting material where Al ion is surrounded by organic molecules-ligands where molecules are π -conjugated. Most studied OS material is 3,4,9,10-perylenetetracarboxylic dianhydride (PTCDA) whose

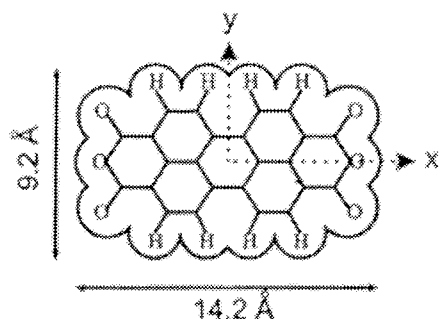


Figure 1: Schematic representation of a single molecule of 3,4,9,10-perylenetetracarboxylic dianhydride.

molecule is illustrated in Fig. 1. The core of the molecule represents perylene, at the sides are attached two dianhydride groups. The HOMO-LUMO energy separation is 2.2 eV and the maximum optical absorption occurs at $\sim 550 \text{ nm}$. This is a hole-conducting material in which carriers are transported predominantly along the direction perpen-

dicular to the molecular planes, where the overlap between p-orbitals of the perylene core and dianhydride groups is the greatest $/3/$.

PTCDA thin films are readily fabricated by vacuum evaporation. The molecules orient themselves parallel to the substrate surface and form monoclinic crystallites whose size depends strongly on the evaporation conditions. Under ultrahigh vacuum and low substrate temperature PTCDA grows almost epitaxially. High vacuum and elevated temperatures on the other hand yield grain size on the order of 50 nm.

2.1. Device physics

The electronic properties of OSs are characterized by molecular levels rather than by the extended bands of delocalized states. However, to illustrate the basic operating principles of an OLED we will use most of the concept derived from the inorganic physics, and keep in mind the peculiarities of OSs. In Fig. 2. we show schematically the basic steps involved in light generation from a single layer of OS by electrical excitation – electroluminescence. The solid lines in the figure represent electronic energy levels although we stress again that typically no delocalized states are present in these materials. As we apply the bias on the structure consisting of a single OS layer sandwiched between two dissimilar metals several processes are underway. The carriers are injected from the electrode, transported along the organic material and captured. They recombine with the oppositely charged particles and consequently the light quanta are emitted

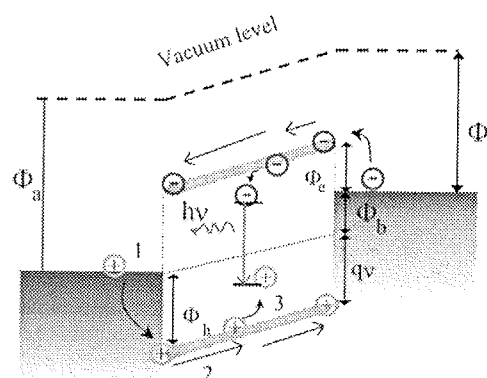


Figure 2: Processes involved in light emission from an organic semiconductor sandwiched between two metallic layers. (1) charge carrier injection, (2) transport across the organic semiconductor, (3) exciton formation, $(h\nu)$ radiative recombination. Indicated are Φ_a and Φ_b , workfunctions of the anode and cathode, respectively, Φ_h and Φ_e hole and electron injection barriers, respectively and $qv = qV - \Phi_b$, where Φ_b/q represents the built-in voltage as a consequence of dissimilar workfunctions of the two metals.

The carrier injection proceeds via the metal/OS interface. If we neglect the interface dipole that may arise due to the charge distribution, and assume the alignment of the vacuum levels across the complete structure we could consider that the interface energy barriers for carrier transport are determined by the metal work functions. This approach is valid only as a first approximation. The metal/OS interface are frequently characterized by defects that stem from disordered growth and/or impure source materials. In addition relatively low-density structure of OS thin films facilitates diffusion of metal atoms yielding chemically intermixed interfaces. Consequently relatively large interface dipoles characterize metallic contacts on OSs, and present additional difficulties in quantitative description of electronic transport.

Injected carriers start their way across the sample under the applied electric field. The transport is markedly different than in the case of inorganic semiconductors. The principal characteristic of OS thin films is comparatively high degree of structural disorder which results in the loss of periodicity. Consequently, the electronic wave function become localized. The charge carrier transport is best described by hopping between these states that are arranged in a spatial array with a given energy distribution. Such transport mode is relatively slow and results in carrier mobilities that are several orders of magnitude lower than those in inorganic semiconductors. In addition, impurities within the OS may introduce energy levels that are lower than the levels in the manifold of hopping states. Such levels act as traps that can immobilize the carriers for longer periods of time.

When the injecting electrode forms Ohmic contact with OS layer and the applied bias is sufficiently high, the density of the injected carriers may exceed the density of the carriers that material can transport. The net charge resides within the OS forming a space-charge, which limits the current across the layer. The space-charge-limited (SCL) current is the maximum current that can flow across the OS layer at a given electric field, unless the opposite contact is capable of injecting the carriers of the opposite sign. The SCL current exhibits a power law dependence on the applied electric field:

$$j \propto E^{l+1} / L^l \quad (1)$$

where E is the electric field and L is the OS layer thickness. In the absence of deep traps $l = 1$, resulting in Child's law seen already in the vacuum tubes. In reality trapping is always present with a given energy distribution of trapping states. In this case the SCL current is best described with $l > 1$, with typical values of 5.

In order to obtain light from the active OS layer the carriers of the opposite sign must recombine radiatively. Due to the low carrier mobility the recombination of electron-hole pairs (excitons) is diffusion-limited and may exhibit radiative or non-radiative character. The probability and the

multiplicity of radiative exciton decay is determined by its spin-symmetry. During electrical excitation approximately one singlet (total spin $S=0$) exciton is created for every three triplet ($S=1$) excitons [2]. Typically only relaxations of singlet excitons conserve spin and generate fluorescence. With disruption of symmetry triplets may slowly radiatively decay resulting in phosphorescence. Phosphorescence was considered inefficient mode of luminescence in OS. Recently the Princeton group demonstrated that the phosphorescence may be enhanced by doping the phosphorescent material with the fluorescent acceptor [2]. The result was an increase in quantum efficiency by a factor of three relative to the undoped material.

2.2. Metal-OS contacts

Metallic contacts on organic semiconductors (OS) are important due to their role in carrier injection in novel organic optoelectronic devices, and successful application of a given metal/OS contacts as a constituent of a device requires precise knowledge of its electrical properties. The alignment of the electronic energy levels across the metal/organic interface determine its transport properties. Electronic properties of the metal/OS interfaces have been examined on a case of prototypical OS 3,4,9,10-perylene-tetracarboxylic dianhydride (PTCDA) by Hirose *et al.* [4,5] using synchrotron radiation photoemission (SRPES). Their findings show that the alignment of the electronic energy levels is strongly dependent on chemical and/or structural abruptness of the interface. Chemically abrupt interfaces are characterized by the interface energy barrier that is determined primarily by the position of Fermi level at the PTCDA surface. Chemically reacted interfaces, on the other hand, exhibit gap states that assist charge carrier transport across the interface and consequently yield ohmic contacts.

First ionization energy of the metal atom appears to be decisive parameter that determines whether a given metal/OS interface acts as a blocking contact or as an ohmic contact [4,5]. Indium is one of the metals with the lowest first ionization energy (5.79 eV) forming ohmic contact to PTCDA. The diffusion of In across the In/PTCDA interface has been thoroughly studied, albeit only for the case of In on highly ordered thin PTCDA layers [4, 8]. Upon arrival of In atoms onto PTCDA surface a formation of a coordination compound In_4PTCDA has been proposed [6,7], and theoretical calculations of its molecular energy structure yielded the states in the gap of PTCDA acting as promoters of the charge carrier transport. Diffusion of In in PTCDA may be different in the case of reversed interface, i.e. PTCDA on In, which is interesting also from the applied standpoint. Also the stability of the interface relative to the increased temperature is of considerable interest for device processing.

We have employed transport measurements coupled to the SRPES experiments to examine the diffusion of In in PTCDA at elevated temperatures. Our results show that

as the temperature of a Ag-PTCDA-In structure approaches the melting point of the In substrate the room-temperature rectifying current-voltage characteristics changes to ohmic. This process transformation is a result of strong In diffusion that is likely to be grain-boundary directed process.

2.2.1. Experimental

The samples for SRPES were synthesized in a vacuum chamber with the base pressure of 1×10^{-6} Torr. The source material was commercially available PTCDA that was purified by evaporating twice onto a collecting shutter that was placed above the Mo boat. We employed Si(001) substrates that were chemically cleaned using RCA etch, followed by dipping in 10% hydrofluoric acid to obtain atomically flat hydrogen-terminated Si(001) surface. Onto such surface we evaporated 1 μm -thick layer of In. During Indium evaporation the substrate was at room temperature (RT). Upon completion of In deposition 1 μm -thick PTCDA layers were grown using a growth rate of 1 nm/s. The layer thickness was monitored using an in-situ quartz thickness monitor. Upon completion of the OS growth we transferred the samples into the analysis chamber that was attached to the 6m-toroidal-grating monochromator beam line of the Synchrotron Radiation center storage ring in Stoughton, Wisconsin. Photoelectron spectroscopy was performed using a cylindrical-mirror analyzer and photon energy ranging from 20 to 130 eV, resulting in the overall resolution of the set-up (electrons+photons) better than 0.25 eV. The samples were mounted onto a sample holder that enabled heating and cooling of the sample in the range of temperatures between 80K and 673K.

The samples employed in transport measurements were identical to the samples investigated by SRPES with the exception of a 100 nm-thick Ag topmost contact, with the effective area of 4.9 mm^2 . The current-voltage (I-V) characteristics measurements were performed using thin In tips attached to the contacts using precision manipulators. We used a Keithley 2400 SourceMeter as a voltage supply and as an ampere meter.

2.2.2 Results and discussion

Our electronic transport data on Ag/PTCDA/In heterostructures agree well with the findings by Hirose *et al* [4,5]. Typical I-V characteristic for a structure comprising 1 μm -thick PTCDA layer grown on In-covered Si(001) and contacted with Ag layer is shown in Fig. 3. The forward current (filled circles) follows a linear dependence for voltages below 0.9V. Beyond that value a power-law dependence on the applied voltage was observed. The power increased from 3.2 to up to 5.9, indicating substantial effect of traps [9] on the electronic transport. Relatively large reverse leakage current (open circles) may be due to image-charge lowering of the Ag-PTCDA interface energy barrier and/or tunneling through the barrier [10]. On the other hand, metals with low ionization potential such as In and Al form ohmic contacts on PTCDA. This is exemplified in Fig. 4(a) where we show an I-V characteristic of an In/PTCDA/In hetero-

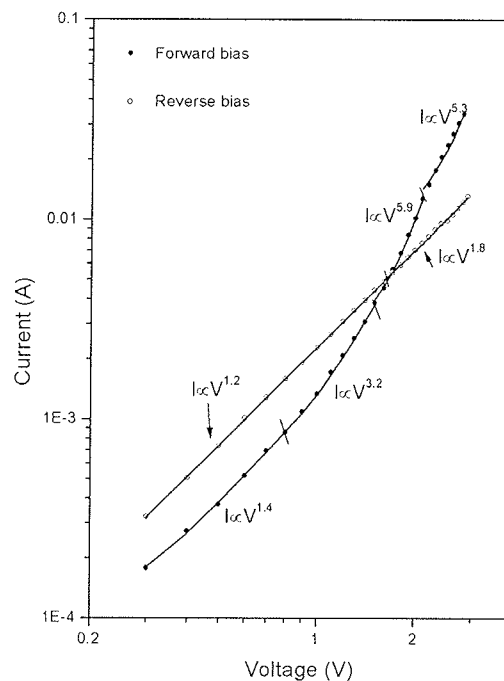


Figure 3: Current voltage characteristic of a Schottky diode comprising 1 μm -thick PTCDA layer evaporated on In-covered Si(001) substrate and contacted to Ag layer. Open circles: reverse bias, filled circles: forward bias. The solid lines represent a least-squares fit to the function proportional to the power of applied voltage. The fitting parameters used in the fit were power exponent and the proportionality factor.

ostructure that was synthesized by evaporation 1 mm-thick In layer onto PTCDA surface. We see a linear dependence that yields the resistance of a complete structure to be 9.4 Ω .

Ohmic character of the In/PTCDA interface is supposedly originating from the interface states that are a consequence of chemical reaction between In and carboxylic groups of PTCDA molecules. According to the recently published work by Ueno and coworkers [8], In atoms, presumably due to the low ionization potential, cede electrons to the PTCDA matrix and form In_4PTCDA coordination compound. Their calculations within the framework of hybrid Hartree-Fock/density functional theory indicate that In_4PTCDA complexes exhibit electronic energy states that lie above HOMO of PTCDA. Such states therefore, act favorably for the charge carriers crossing the In-PTCDA interface [4,5]. The linear I-V characteristic presented in Fig. 4(a) indicates that the chemical reaction leading to the formation of interface states takes place when free In atoms arrive onto the PTCDA surface, as well as when In atoms are bound in the metallic substrate. This results in the two interfaces characterized by a region where In diffusion determines their ohmic character.

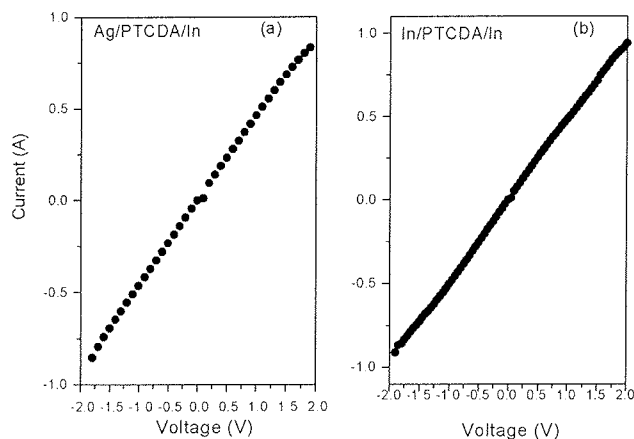


Figure 4: (a) Current-voltage characteristic of a structure comprising 1 μm -thick PTCDA layer evaporated on In-covered Si(001) substrate and contacted to In layer. Both metallic layers form a conductive contact to PTCDA. (b) Current-voltage characteristic of a structure comprising 1 μm -thick PTCDA layer evaporated on In-covered Si(001) substrate and contacted to Ag layer, after heating to 120 $^{\circ}\text{C}$.

Diffusion of In may assume drastic proportions if the sample is heated to 120 $^{\circ}\text{C}$ or above. The effect is illustrated by comparing Fig. 3 to Fig. 4(b), where we show the I-V characteristic of the sample used to obtain the data in Fig. 3, after heating to 120 $^{\circ}\text{C}$. We see a dramatic change from rectifying to ohmic. Based on the I-V characteristic alone we can not rule-out the possibility that both In and Ag species diffuse into PTCDA, however our SRPES measurements indicate that In diffusion at elevated temperatures is extremely strong, resulting in In-related species diffusing through PTCDA layers as thick as 1 μm .

We demonstrate this by Fig. 5, which shows the photoelectron energy distribution curves (EDCs) measured on 1 μm -thick PTCDA layer grown on In-covered Si(001) substrate. Individual curves correspond to the sample at RT (bottom-most curve) and 150 $^{\circ}\text{C}$ (topmost curve).

The curves were obtained using photon energy of 80 eV. The binding energy scale is referenced to the position of the Fermi level that was determined from the photoemission cut-off of an in situ sputter-cleaned copper foil. We observed features in increasing binding energy that are pertinent to different energy levels of a PTCDA molecule /6-12/.

As the temperature of the sample increased to 150 $^{\circ}\text{C}$ we observed a strong emission of In 4d core level (topmost EDC). Room-temperature In diffusion can be ruled out based on the results illustrated in the inset, showing an EDC obtained with photon energy of 130 eV on 1 μm -thick PTCDA layer grown on clean Si(001) substrate. The feature at the binding energy of about 20 eV is present also in

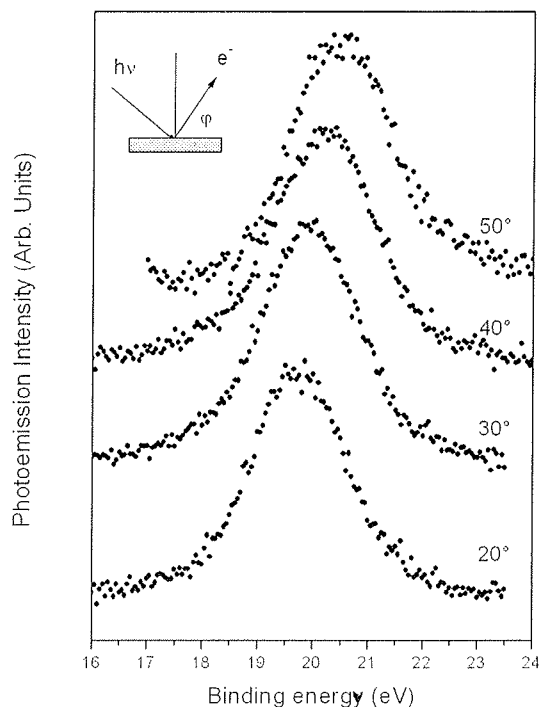


Figure 6: Photoelectron energy distribution curves of a PTCDA/In/Si(001) structure indicating In diffusion as a consequence of sample heating. The photon energy employed was 80 eV. The curves represent emission from the sample at room temperature, and 150 $^{\circ}\text{C}$, bottom to top, respectively. The narrow feature observed in the topmost curve corresponds to the emission from the In 4d core level. Inset: the photoelectron energy distribution curve from a PTCDA/Si(001) sample. The feature at 19.8 eV seen in this curve is originating from PTCDA and not from In

this EDC and must therefore reflect the emission from the PTCDA-related energy states. From Fig. 5 we see that although the In-PTCDA chemical reaction takes place even if In atoms are bound in metallic In polycrystal, the room-temperature intermixing does not reach the surface of the 1 μm -thick PTCDA layer. When the sample temperature reaches or exceeds the melting temperature of In however, substantial In-related photoemission is observed. From the position and lineshape analysis of the In 4d emission we can obtain the information on the chemical nature and consequently diffusion mechanism of In in PTCDA.

The emission from the In 4d core level presented in the topmost curve of Fig. 5 is relatively broad, which indicates a wealth of different chemical environment that In atoms may encounter upon diffusing towards the PTCDA surface. To check if the chemical environment of In atoms changes with the distance from the surface we have performed angular-dependent measurements, where we varied the emission angle (ϕ) from grazing towards normal. The incident angle of the photons also varied as $(\pi/2 - \phi)$. The results

are exemplified in Fig. 6, where we show the background-subtracted measurements as a function of emission angle (increasing bottom to top). The featureless lineshapes precludes reliable numerical analysis, although we have attempted to extract individual contributions to the observed emission. Note that the apparent binding energy of the feature presented in Fig. 6 deviates considerably from the published data for In 4d core emission in metallic In as well as for In 4d in compound semiconductors. For example, the positions of the In 4d_{5/2} and In 4d_{3/2} doublet components are reportedly 16.35 eV, and 17.25 eV, respectively /16/ determined by SRPES on the polycrystalline film evaporated *in situ*. For the InSb these values are chemically shifted to 17.0 eV, and 17.8 eV, respectively /16/. Bermudez and Ritz /17/ observed by SRPES a 0.7 eV shift of the In 4d core-level emission centroid upon oxidation of the InSb(110) surface, and Sen *et al* report on the XPS-derived 1.1 eV chemical shift in In 4d centroid in In₂O₃ relative to the In 4d in polycrystalline film /18/. We attribute this variance to the final-state effects. Screening of the In core-hole is considerably less efficient for In atoms embedded in PTCDA matrix relative to that in In metal on In-compound semiconductors /4, 5/. The centroid of the peak monotonically moves from 19.76 ± 0.05 eV to 20.59 ± 0.05 eV, for 20° and 50°, respectively. Coupled to this shift we observe an increase in FWHM of the peak from 1.9 eV to 2.18 eV for 20° and 50°, respectively. We interpret this behavior in a qualitative fashion in terms of multiple chemical environment of In atoms that vary with depth from the surface. The estimated photoelectron escape depth at these kinetic energies is ~4 Å /14/. Assuming that the photoemission signal is coming from roughly three times the escape depth, and taking into account that the molecules stack parallel to the substrate surface with the inter-

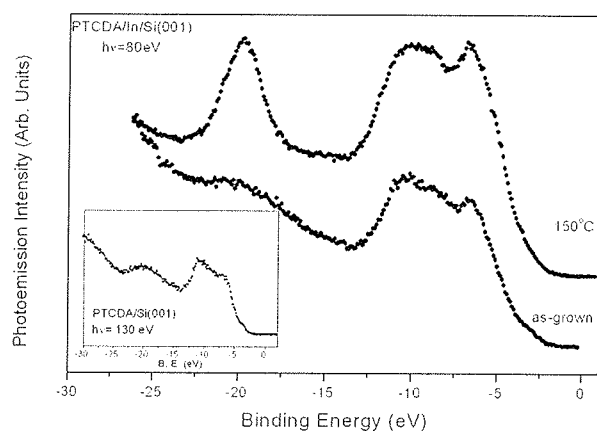


Figure 5: In 4d core level photoelectron energy distribution curves obtained at different emission angles indicated at the left side of each curve. The binding energy scale is referenced to the spectrometer Fermi level. Inset: The emission angle in the figure is defined as the angle between the longer axis of the analyzer and the projection of this line on the sample surface.

molecular separation of 3.21 Å /15/, we see that by changing the emission angle from 20° to 50° we have probed the region from the topmost molecular layer to the third molecular layer below the surface, respectively. At grazing emission the spectrometer detects photoelectrons only from the topmost molecular layer. The smallest FWHM of the peak indicates the presence of fewer In-related species; perhaps indium oxide and metallic In. As the emission angle increases towards normal the contribution of high-binding-energy component strongly increases, causing a high-binding-energy shift of the peak centroid coupled to the increase in FWHM. Large high-binding-energy shift (0.83 eV) suggests that the abundance of low-binding-energy component residing on the surface is relatively small. We can only speculate on the possible chemical environment of In atoms that contribute to the observed emission.

Apart of the metallic In and two common In oxides, InO and In₂O₃, In₄PTCDA comes to mind as possible candidate to explain the observed depth dependence of the In 4d core emission. We have evidence, however that the latter compound is not present at the PTCDA surface, when In atoms are subjected to diffusion through the layer of PTCDA. The signature for In₄PTCDA are the energy states above HOMO in PTCDA /6, 7/. In Fig. 7 we show the EDCs obtained on the same sample as those in Fig. 5; this time with the photon energy of 50 eV. Focusing on the region near HOMO we see no emission Fermi energy and HOMO at the sample temperature of 150 °C, when we observed a strong In 4d core emission. Based of this evidence we can rule out the interaction of In with PTCDA in the form pro-

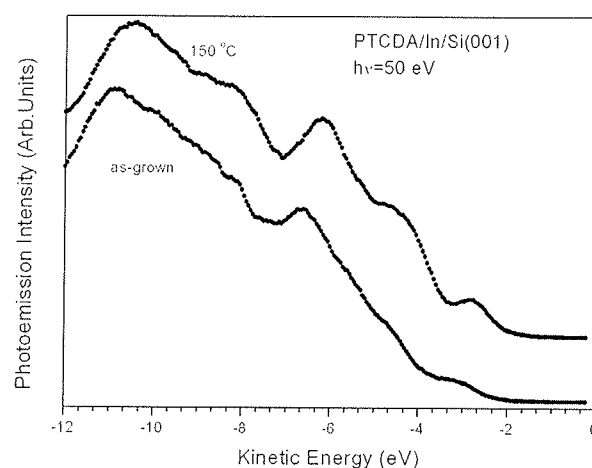


Figure 7: Energy distribution curve taken at increasing temperatures of the 1 μm-thick PTCDA layer grown on In-covered Si(001). The energy scale is referenced to the spectrometer Fermi level. The bottommost curve was obtained on the as grown sample, to the bottommost curve in Fig. 5. The topmost curve was obtained after heating of the sample to 150°C, and corresponds to the topmost curve in Fig. 5. The photon energy employed was 50 eV.

posed by Ueno and co-workers /6,7/, when In is coming from In substrate.

The mechanisms connected to In diffusion are therefore different when PTCDA is evaporated onto In substrate than the mechanisms connected to In diffusion in the case of In evaporation onto ordered PTCDA surface. The tentative explanation assumes the formation of In_4PTCDA as the PTCDA molecules arrive onto In surface. The formation of the coordination compound is limited to the initial layer of thickness of few hundred Å /4,5/, and is determined by the room-temperature diffusion rate of In in PTCDA. Upon formation of sufficiently thick interface layer, the growth continues in the form of PTCDA. When the sample is heated the diffusion of In from the substrate is enhanced. The structure of the PTCDA overlayer is crucial for the diffusion.

Indium layer evaporated on Si(001) acts as structurally considerably different template for the PTCDA growth than the substrates employed in previous reports where atomically clean semiconductor /5-12/ or MoS_2 substrates were used /6,7/. Indium in thin film form is prone to three-dimensional island formation. Spicer and co-workers /19/ examined the growth of In on GaAs(110) substrates. Their SRPES results indicate that In forms atomic clusters for nominal coverage up to 8 monolayers, resulting in a discontinuous coverage. Ryu *et al.* /20/ examined In overlayers on hydrogen-terminated Si(001) substrates at different coverage by scanning tunneling microscopy (STM). After the thickness of In exceeds several monolayers (ML) the two-dimensional islands start to evolve into three-dimensional columns. Since the thickness of our In layers was 1 μm , we may safely assume that the surface exhibited increased roughness relative to the atomically flat hydrogen-passivated Si(001). In addition to the polycrystalline substrate, the PTCDA layer thickness and room-temperature of the substrate suggest that our PTCDA layer is polycrystalline /21/. High concentration of grain boundaries enhances a grain-boundary diffusion. Grain boundaries are also likely to contain embedded oxygen molecules, whereas the outermost layer of the film is oxygen-free due to oxygen desorption at elevated temperatures. Given the affinity of In to form oxides at temperatures that approach its melting point it is likely that the majority of In atoms remain immobilized as In_2O_3 and/or InO , and only few In atoms manage to reach the surface in atomic form, where they contribute to the low-binding-energy photoelectron emission presented in the bottommost curve of Fig. 6. The high-energy component of the EDCs shown in Fig. 6 might therefore represent the emission from In atoms in In_2O_3 . Relatively fast decrease in intensity with the emission angle indicates low probability for In atoms to diffuse to the surface without forming an oxide.

3. Conclusion

In-PTCDA interface retains its ohmic character regardless the order of the layers, i.e. In on PTCDA or PTCDA on In. Diffusion of In in PTCDA at elevated temperatures, depends

on the order of the layers and is likely to proceed via a grain-boundary network when polycrystalline PTCDA is grown on In substrates. Angular resolved photoemission reveals differences in chemical environment of In atoms that reside on the surface of thick PTCDA layers relative to the chemical environment of In atoms that reside in the molecular planes below the surface. Based on the binding energy of the In 4d core-level emission obtained at grazing-angle emission relative to the binding energy at high emission angle we suggest that small concentration of metallic In occupies sites on the PTCDA surface.

4. References

- /1/ C. W. Tang, et al. "Electroluminescence of doped organic thin films", *J. Appl. Phys.* vol. 65, pp. 3610-3616 1989,
- /2/ M. A. Baldo *et al.* "High-efficiency fluorescent organic light-emitting devices using a phosphorescent sensitizer", *Nature*, vol. 403, February 2000, pages 750-753, and references therein.
- /3/ For a review on material properties and synthesis see: Stephen R. Forrest, "Ultrathin organic Films Grown by organic Molecular Beam Deposition and Related Techniques", *Chem. Rev.* vol. 97, 1997, pages 1793-1896, and references therein.
- /4/ Y. Hirose, A. Kahn, V. Aristov, P. Soukiassian, V. Bulovic, and S. R. Forrest, "Chemistry and electronic properties of metal-organic semiconductor interfaces: Al, Ti, In, Sn, Ag, and Au on PTCDA", *Phys. Rev. B*, 54, 19, November 1996, 13748-13758.
- /5/ Y. Hirose, A. Kahn, V. Aristov, and P. Soukiassian, "Chemistry, diffusion, and electronic properties of a metal/organic semiconductor contact: In/perylene-tetracarboxylic dianhydride", *Appl. Phys. Lett.*, 68, 2, January 1996, 217-219.
- /6/ S. Kera, H. Setoyama, M. Onoue, K. K. Okudaira, Y. Harada, and N. Ueno, "Origin of indium-[perylene-3,4,9,10-tetracarboxylic dianhydride] interface states studied by outermost surface spectroscopy using metastable atoms", *Phys. Rev. B*, 63, 11, March 2001, 115204-115211.
- /7/ Y. Azuma, T. Hasebe, T. Miyamae, K. K. Okudaira, Y. Harada, K. Seki, E. Morikawa, V. Saile, and N. Ueno, *J. Synch. Radiation* 5, 1044 (1998);
- /8/ Y. Azuma, S. Akatsuka, K. K. Okudaira, Y. Harada, and N. Ueno, "Angle-resolved ultraviolet photoelectron spectroscopy of In-[perylene-3,4,9,10-tetracarboxylic dianhydride] system," *J. Appl. Phys.*, 87, 2, January 2000, 766-769.
- /9/ Amarjit Singh, "Electrical conduction and trapping distributions in tellurium oxide films", *Phys. Rev. B*, 37, 17, June 1988, 10371-10373.
- /10/ S. R. Forrest, M. L. Kaplan, and P. H. Schmidt, "Organic-on inorganic semiconductor contact barrier diodes. I. Theory with applications to organic thin films and prototype devices," *J. Appl. Phys.*, 55, 6, March 1984, 1492-1507.
- /11/ S. M. Sze, *Physics of Semiconductor Devices*, 2nd Ed., Wiley, New York, 1981, 0-471-05661-8.
- /12/ S. R. Forrest, M. L. Kaplan, and P. H. Schmidt, "Organic-on inorganic semiconductor contact barrier diodes. II. Dependence on organic film and metal contact properties," *J. Appl. Phys.*, 56, 2, July 1984, 543-551.
- /13/ M. Jung, U. Baston, G. Schnitzler, M. Kaiser, J. Papst, T. Porwol, H. J. Freund, and E. Umbach, "The electronic structure of adsorbed aromatic molecules: Perylene and PTCDA on Si(111) and Ag(111)", *J. Molecular Struct.* 293, 1993 239-244.
- /14/ T. Kendelewicz, P. H. Mahowald, K. A. Bertness, C. E. McCants, I. Lindau, and W. E. Spicer, "Surface shifts in the In 4d and P 2p core-level spectra of $\text{InP}(110)$," *Phys. Rev. B*, 36, 12, October 1987, 6543-6546.

- /15/ D. Y. Zang, F. F. So, and S. R. Forrest, "Giant anisotropies in the dielectric properties of quasi-epitaxial crystalline organic semiconductor thin films," *Appl. Phys. Lett.*, 59, 7, August 1991, 823-825.
- /16/ G. Margaritondo, J. E. Rowe, and S. B. Christman, "Photoionization cross section of d-core levels in solids: A synchrotron radiation study of the spin-orbit branching ratio", *Phys. Rev. B*, 19, 6, March 1979, 2850-2855.
- /17/ V. M. Bermudez and V. H. Ritz, "Oxygen adsorption on the indium antimonide (110) surface," *Phys. Rev. B*, 26, 6, September 1982, 3297-3308.
- /18/ P. Sen, M. S. Hedge, and C. N. R. Rao, "Surface Oxidation of Cadmium, Indium, Tin and Antimony by Photoelectron and Auger Spectroscopy", *Appl. Surf. Sci.* 10, 1982, 63-74
- /19/ Perry Skeath, I. Lindau, C. Y. Su, and W. E. Spicer, "Chemical bonding, adatom-adatom interaction, and replacement reaction of column-3 metals on GaAs(110)," *Phys Rev. B*, 28, 12, December 1983, 7051-7067.
- /20/ J.T. Ryu, O. Kubo, H. Tani, T. Harada, M. Katayama, and K. Oura, "The growth of indium thin films on clean and hydrogen-terminated Si(100) surfaces," *Surf. Sci.*, 433-435, August 1999, 575-580.
- /21/ S. R. Forrest, P. E. Burrows, E. I. Haskal, and F. F. So, "Ultra-high-vacuum quasiepitaxial growth of model van der Waals thin films. II. Experiment", *Phys. Rev. B*, 49, 16, April 1994, 11309-11321.

G. Bratina and R. Hudej
Nova Gorica Polytechnic,
Vipavska 13, POB301,
5001 Nova Gorica

Prispelo (arrived): 10.09.01

Prejeto (Accepted): 01.10.01